Investigating the effect of CuO loadings on TiO$_2$ nanocomposite photocatalysts (0-8 w/w%) on pseudo first order rate constants (k) for the rate of agricultural Cypermethrin decomposition

Jishnu Talukdar

E-mail: talukdar.jishnu@gmail.com

Abstract

Cypermethrin, a common agricultural insecticide, often pollutes aquatic environments through soil sediment runoff or excess spraying onto water surfaces. Cost-effective CuO/TiO$_2$ heterojunction photocatalysts were investigated as a means of using sunlight to decompose cypermethrin into non-toxic byproducts. CuO/TiO$_2$ of various loadings (1,2,4,6 and 8 w/w%) were synthesised via precipitation. They were characterised using the Tauc method and Ultraviolet-Visible (UV-Vis) Spectroscopy. Then, they were mixed into aqueous solutions of dissolved cypermethrin and exposed to 324nm ultraviolet light. Cypermethrin concentrations in these reacting solutions were tracked over time through UV-Vis Spectroscopy. Cypermethrin's rate of photodecomposition was found to follow the pseudo first order reaction model. An increase in CuO loading corresponded with a higher pseudo first order rate constant (k) from 0-2w/w%, peaking at 2 w/w%. Subsequent increases in CuO loadings (4-8 w/w%) resulted in a drop in the k. By analysing CuO/TiO$_2$ catalyst characterisation data, it was identified that higher CuO loadings further reduced the activation energy for cypermethrin decomposition, increasing its rate and thus k. However, CuO loadings that were too high may have caused CuO to accumulate on the TiO$_2$ surface, inhibiting the catalyst's efficacy and thus cypermethrin decomposition rate. Therefore, the balance between reducing activation energy and affecting TiO$_2$'s surface area was found at 2 w/w% loading, resulting in the highest rate of cypermethrin decomposition.

Keywords: Cypermethrin, nanocomposite, photocatalyst, heterojunction, water pollution

1. Introduction

1.1 Cypermethrin Toxicology

Cyano-(3-phenoxyphenyl)methyl]3-(2,2-dichloroethenyl)-2,2-dimethylcyclopropane-1-carboxylate (Cypermethrin) is an insecticide commonly used agriculture and home insect control (Chrustek, et al., 2018). It has increased in popularity over the years due to its relative safety compared to alternatives like chlorinated hydrocarbon, carbamate, or organophosphate insecticides (K.Malik, et al., 2017).

Despite this relative safety, when spread to non-target environments like water bodies near agricultural areas, cypermethrin is still highly toxic to fish and other aquatic invertebrates (R.R.Stephenson, 1982), causing imbalances in aquatic ecosystems (LWendt-Rasch, et al., 2003). Even in humans, consuming this polluted water can cause severe pyrethroid poisoning; and long-term exposure can impair immunity, cause dangerous gene mutations and induce functional cell oxidative stress (Chrustek, et al., 2018).

Cypermethrin water pollution occurs especially due to poor management in the agricultural sector: it is often exposed to aquatic environments by pesticide in soil sediment runoff (W., et al., 2018) as cypermethrin has a relatively long half-life in soil of 2 to 4 weeks (Chapman, et al., 1981) or more; and excess spraying onto water body surfaces. Therefore, toxicity spikes are frequently observed in streams draining into agricultural basins (Mugni, et al., 2011). Therefore, there is a dire need to find a low cost method for agricultural cypermethrin removal.

1.2 Previous Investigations on Cypermethrin removal

The toxicity of cypermethrin can be significantly reduced through its decomposition into less toxic products ((IPCS), 1989). Previous investigations have taken advantage of this property in finding cypermethrin removal methods: biotic methods involving microorganisms (Cycoń & Piotrowska-Seget, 2016) and enzyme availability; and abiotic methods involving soil pH and exposure to electromagnetic radiation (Jones, 1995).

Of these methods, one of the most realistically applicable is the use of electromagnetic radiation in the breakdown of cypermethrin.

1.3 Photocatalytic Decomposition

When exposed to sunlight in the absence of photocatalysts, cypermethrin uses multiple pathways of photodegradation such as de-chlorination, phenyl group removal, ester bond cleavage, decarboxylation or more (Xie, et al., 2011), depending on reacting conditions inclusive of pH and oxidising agents present.

Various photocatalysts like hydrogen peroxide, ozone and titanium dioxide (TiO_2) have investigated in accelerating the photo-decomposition of cypermethrin, where UV lamp irradiation is often used to simulate sunlight under laboratory settings (Lina, et al., 2012).

However, hydrogen peroxide and ozone on their own are not only toxic, but also expensive, making them unrealistic in the agricultural context. On the other hand, TiO_2 and its various nanocomposites (Chioma, et al., 2013) are comparatively low-cost, non-toxic, and can be added easily to soil as a solid powder.

TiO_2 is an effective photocatalyst as its band gap, the energy gap between the valence band and conductor band of the solid (Connor, 2019), is between 3.0-3.2eV (Michael Dahl, 2014). When it is illuminated by photons of light with energy which exceeds its low band gap, electrons (e^-) in the valence band get excited and rise to the conduction band, also

producing holes (h^+) in the valence band as shown in equation 1 (Chioma, et al., 2013).

| Equation 1	$$TiO_2 + hv \rightarrow TiO_2(e^- + h^+)$$
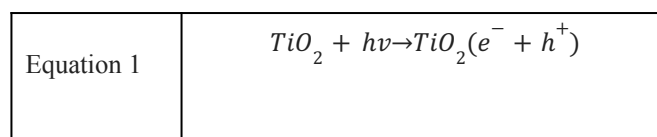
These charges then migrate to the surface of the TiO2 solid (Michael Dahl, 2014), enabling the following redox reactions to occur (equation 2,3): (Chioma, et al., 2013).

Equation 2	$$h^+ + H_2O \rightarrow OH^. + H^+$$
Equation 3	$$h^+ + OH^- \rightarrow OH^.$$
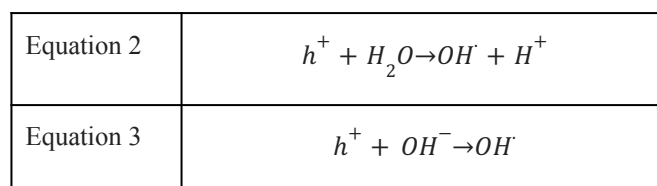
The hydroxyl radicals are highly reactive and enable the splitting of cypermethrin as shown in fig 1 (Al-Shuja'a, et al., 2013); where A is cypermethrin and the hydroxyl radical cleaves the ester group, resulting in a carboxylic acid and ether.

Figure 1: Mechanism of decomposition of cypermethrin (Al-Shuja'a, et al., 2013); A is a molecule of cypermethrin.
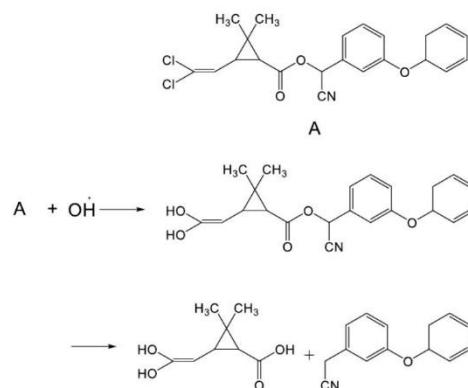
However, TiO_2 as a catalyst on its own may be insufficient to incur a large enough removal rate of cypermethrin, especially in the realistic and unideal conditions of agricultural soil solution. Therefore, to enhance the efficacy of TiO_2, it is possible to form heterojunctions of it and another substance, usually a metal or metal oxide to form a more effective composite photocatalyst.

Past studies have investigated Zinc and Aluminium and their oxides' composites with TiO_2 as photocatalysts with some success, often reaching 60-70% or above rates of cypermethrin removal (Rusmidah Ali, 2010), recent studies with Iron composites have even reached a maximum of 100% cypermethrin removal rates (Pizarro & Barros, 2020).

However, these studies often involve optimal conditions which would be unrealistic under actual agricultural conditions of soil solution, and require the use of reactive metals in the formation of said catalysts. Reactive metals like Iron, Aluminium and Iron are expensive to obtain is large amounts and the process to make the TiO_2 heterojunction catalysts are also likely expensive.

This investigation thus explores the cost effective alternative – Copper oxide, in the formation of the CuO/TiO_2 heterojunction photocatalyst. Little to no studies have been conducted on the effect of CuO/TiO_2 on the decomposition of cypermethrin, making this investigation essential. CuO has a low band gap of 1.4 eV, making it highly desirable for conversion of solar radiation (Michael Dahl, 2014), applicable to natural light induced decomposition of cypermethrin, known for the significant improvement of the photocatalytic ability of TiO_2 when the heterojunction catalyst is formed.

2. Background

2.1 Quantifying Cypermethrin concentration

To quantify the efficacy of a TiO_2 nanocomposite photocatalyst, its effect on the rate of cypermethrin decomposition must be found. To do so, a quick method for determining cypermethrin concentration in a solution is essential.

The halogenation of the vinyl group in cypermethrin's cyclopropane ring (Palmquist, et al., 2011) allows it absorb light within the visible range (Alemán, 2017). Additionally, cypermethrin follows the Beer Lambert's Law (Shaheed & Dhahir, 2020).

Thus, UV Visible spectroscopy with a maximum absorbance occurring at $\lambda_{maximum}$ =208 nm (Al-Shuja'a, et al., 2013) was be used to quickly find its concentration in a solution.

2.2 Solvents for Cypermethrin

Cypermethrin is insoluble in water ((IPCS), 1989), but water is required for photodecomposition in the presence of TiO2 to occur so as to enable the formation of hydroxyl radicals. Therefore, a cosolvent which enables cypermethrin to dissolve in water is necessary.

Acetonitrile is a common cosolvent for cypermethrin, but it is highly flammable and liberates toxic hydrogen cyanide fumes at higher temperatures (health, revised 2005), thus it is too dangerous to be used in a school lab setting. The alternative ((IPCS), 1989), ethanol is used due to cypermethrin's high solubility in it, along with the miscibility

of ethanol in water, ensuring that it acts as a good cosolvent. The ratio of ethanol to water in reacting solutions is determined through section 3.1.

2.3 Quantifying Cypermethrin purity

Agricultural cypermethrin solution (Anon., n.d.) is used for this investigation as it enables a realistic simulation of its application in agriculture.

Conventionally, the percentage purity of cypermethrin is obtained using two gas chromatography methods –with flame ionization detection (GC-FID) or with electron capture detector (GC-ECD) (Ahmed, et al., 2017). However, due to the lack of such equipment, these methods were not used for this investigation.

Instead, a novel method was used for determining the cypermethrin purity, which exploits the presence of the ester bond in the cypermethrin chemical structure (ref. fig. 1).

Cypermethrin's hydrolysis is catalysed by the presence of dilute sulfuric acid and water, enabling the cleavage of the ester due to the presence of hydronium ions (Yates & McClelland, 1967) when heated under reflux. The reflux heating was conducted in the fume hood due to the liberation of toxic chemicals from the heating the insecticide.

The products of hydrolysis of one mole of cypermethrin results in one mole of carboxylic acid and one mole of 3-phenoxybezaldehyde. A back titration using Sodium Hydroxide (NaOH), Hydrochloric acid (HCl) and bromothymol blue indicator was then used to find out the amount of carboxylic acid produced from the hydrolysis, and thus the concentration of the agricultural cypermethrin solution. A back titration is conducted in place of a traditional acid-base titration because the carboxylic acid is very weak.

2.4 Nanocomposite Synthesis

Of the methods for CuO/TiO_2 synthesis such as the modified oxalate method (Ekane Peter Etape, 2017), electrosynthesis (Ridha, et al., 2020) and neumerous others, the method by Nguyen et. al 2013 is used in this investigation due to its low cost. This is congruent with the objective of this investigation – finding a low-cost method for cypermethrin removal. This is because the method is relatively simple, involving the direct addition of a dilute solution of Copper (II) nitrate solution to TiO_2 dispersed in ethanol, stirring it and raising the pH till precipitate of solid catalyst forms. Unlike the original method however, the concentration of the dilute Copper (II) nitrate solution is varied to create the different loadings of CuO/TiO_2 (1,2,4,6 and 8 w/w% by wt.).

2.5 Nanocomposite Characterization

UV Visible diffuse reflectance spectroscopy can be used for the characterisation of the composites, ensuring that the powdered photocatalysts formed are indeed nanocomposites, rather than merely mixtures of CuO and TiO_2.

The process involves the dispersion of the solid photocatalysts into a solution for UV vis analysis, to find its UV vis absorption spectrum (Stone, 1983). The spectra obtained can also be used to identify the band gaps of each of the composites using the Tuac method (Makula, et al., 2018).

A band gap is the minimum energy required for an electron to transition from the valence band of electrons of the compound, to its conduction band of unfilled orbitals (Gokul Dharan, 2018). In the conduction band, electrons are able to move freely through the material, affecting the material's conductive, electric and catalytic properties (Gokul Dharan, 2018). Anatase TiO_2, used in this investigation, is known to have an indirect band gap transition (Peh, et al., 2017): photons of light at higher energy than the band gap can excite the electrons, forming electron-hole pairs in the compound in the valence band, which indirectly migrate into the conduction band to engage in redox reactions with temporarily adsorbed reactants (Michael Dahl, 2014). In the CuO/ TiO_2 nano composite formed in this investigation, TiO2 forms a shell around CuO to varying degrees depending on the loading affecting the morphology of the TiO_2 catalyst (Michael Dahl, 2014). These changes affect the charge migration (Michael Dahl, 2014) from the valance to the conduction band of the catalyst, causing differences in band gaps. Thus, band gaps can be used as a means to characterise CuO/ TiO_2 catalysts at different loadings.

In the Tauc method, the spectrum scan data is converted to a Tauc Plot using the following equation 4 (Albert Zicko Johannes, 2020):

Equation 4	$(\alpha h v)^{\frac{1}{\gamma}} = B(h v - E_g)$
Constants	
$\alpha = \frac{a \ln \ln (10)}{l}$	a is absorbance and l is path length (1 cm)

h	Planck's constant in electron-volts (eV), 4.135×10^{-15} eV
v	frequency of light in s^{-1}
B	comparative constant
$h v$	the energy of light at the specific wavelength λ, in eV, for which the conversion from Joules to eV can be obtained through $h v = \frac{hc}{\lambda}$ x 6.241509 x 10^{18} eV
γ	2 specifically for anatase TiO_2 used in this investigation (Peh, et al., 2017) due to its indirect electronic transition.

Therefore, in the Tauc plot, (αhv)^(1/γ) is plot against hv, and the linear portion of the curve is extrapolated till it intersects the hv axis. This intersection point is the band gap.

2.6 Cypermethrin decomposition

In the presence of TiO_2 and UV light, and in an aqueous environment which is used to simulate the soil solution, the degradation of cypermethrin is known to follow the pseudo first order (ref. equation 4) kinetic model (Chioma, et al., 2013).

Given that this is a pseudo first order reaction with excess water, the only factor affecting the concentration for each set-up, other than the loading of CuO on TiO_2, is the concentration of cypermethrin.

Thus for further data processing, the rate expression can be shown as follows:

Equation 5	Rate of reaction $=- k$[cypermethrin]

Where k is the first order rate constant; [cypermethrin] is concentration of cypermethrin; and the overall linear expression with respect to time is (Al-Shuja'a, et al., 2013):

Equation 6	$\ln[\text{cypermethrin}] = -kt + [\text{cypermethrin}]_0$

Thus, k can be found through the gradient of the linear plot of ln[cypermethrin] against time in minutes, t, for each set-up (ref section 4.4). This linear correlation coefficient between the concentration and time (R^2) shows the goodness of fit of the reaction to a first order reaction. The half-life of cypermethrin can then also be calculated using $\frac{\ln\ln(2)}{k}$ as this is a first order reaction.

3. Methodology

3.1 Procedure for finding a solvent for Cypermethrin

1.   Measure 1.000 cm3 of agricultural cypermethrin using a 1.000 cm3 pipette

2.   Measure 20.00 cm3 of distilled water using a 20.00 cm3 pipette

3.   Empty both the 1.000 cm3 and 20.00 cm3 pipettes into a 250 cm3 conical flask

4.   Fill a burette with 95% ethanol

5.   Add 95% ethanol from a burette to the solution into the 250 cm3 conical flask while swirling till the solution turns completely clear

6.   Repeat this process on the triplicate

7.   Using the average volume of 95% ethanol required, calculate the optimal water to 95% ethanol ratio. Solutions later made in this ratio of water to ethanol will be referred to as solvent A.

3.2 Procedure for Quantifying Cypermethrin Purity

1.   Make solvent A, but using dilute sulfuric acid (0.01M) instead of water. This acid act as the catalyst for the ester hydrolysis of cypermethrin.

2.   Measure 0.5 cm3 of agricultural cypermethrin using a 0.5 cm3 pipette

3.   Obtain 50 cm3 of solvent A using a 50 cm3 pipette

4.   Dissolve the 0.5 cm3 of agricultural cypermethrin in the 50 cm3 of solvent A. This mixture will be referred to as solution B.

5.   Empty a 20cm3 aquilot of solution B using a 20 cm3 pipette into a round bottom flask in the reflux set-up.

6.   Heat solution B under reflux for 2 hours (Ambrus & Hamilton, 2011). Conduct this reflux experiment in the fume hood.

7.   Wash down the walls of the condenser using distilled water to ensure all of the refluxed solution has fallen back into the round bottomed flask.

8.   Remove the refluxed solution from the round bottom flask, empty it into a 250 cm3 conical flask.

9.   Add 5 cm3 of 2M NaOH measured using a 5 cm3 pipette.

10.   Titrate this solution with 0.25 M HCl from a burette, using bromothymol blue indicator till the end point is reached

11.   Repeat this process to obtain a triplicate

3.3 Procedure for Quantifying Cypermethrin Concentration

1.   Using a 1 cm3 pipette, measure 1 cm3 of agricultural cypermethrin and dissolve it in 60 cm3 of solvent A measured using a thrice emptied 20 cm3 pipette.

2.   Use a dropper to fill up a quartz cuvette with this mixture, and put it into the UV Vis Spectrophotometer

3.   Repeat this process with 0.8, 0.6, 0.4, and 0.2 cm3 of agricultural cypermethrin solution in 60 cm3 of solvent A measured by reusing a 20.00 cm3 pipette.

4.   Find the absorbance through each cuvette at 208 nm light.

5.   Absorbance against concentration is plot to obtain the Calibration curve.

3.4 Procedure for Nanocomposite synthesis (Thi Hiep Nguyen & Nguyen, 2013)

1.   Disperse 1.0g TiO_2 of 250ml of 95% ethanol.

2.   Obtain solution of Copper (II) Nitrate such that it adheres to the eventual CuO: TiO_2 weight ratio of 1 w/w %, to form a 250ml solution of Copper (II) nitrate.

3.   Stir the solution vigorously for 1 hour

4.   Add 0.5M NaOH dropwise till the solution reaches pH 10, track the pH using a pH sensor.

5.   Stir this solution, again for 1 hour using a magnetic stirrer at 250 RPM.

6.   Centrifuge the total solution at 4000 RPM for 15 minutes and obtain the solid pellets.

7.   Rinse the solution using distilled water and absolute ethanol, over a vacuum filter.

8.   Dry the solid obtained in the oven at 60 degrees Celsius for 8 hours

9.   Calcine the solid obtained in the furnace, this will obtain the 1w/w % CuO/TiO$_2$.

10.   Repeat the process to obtain 2,4,6 and 8 w/w % CuO/ TiO$_2$.

3.5 Procedure for Nanocomposite characterization

1.   A mass of 0.02g of solid 1 w/w % CuO/ TiO$_2$ photocatalyst was dispersed separately in 20 ml of ethanol using a sonicator.

2.   Then a UV Vis spectrum scan was conducted on each of the dispersion within the range of 190nm to 900nm (Jiang Wu, 2016)

3.   Repeat the process for 2, 4, 6 and 8& wt. CuO/ TiO$_2$.

4.   Convert each spectrum scan to a Tauc Plot (ref Background).

3.6 Procedure for Cypermethrin decomposition

Figure 2: Rate of reaction set-up

General set-up	

Arrangement of Volumetric flaks	
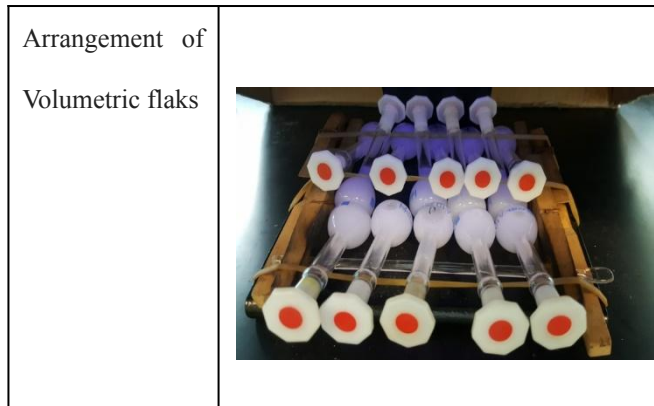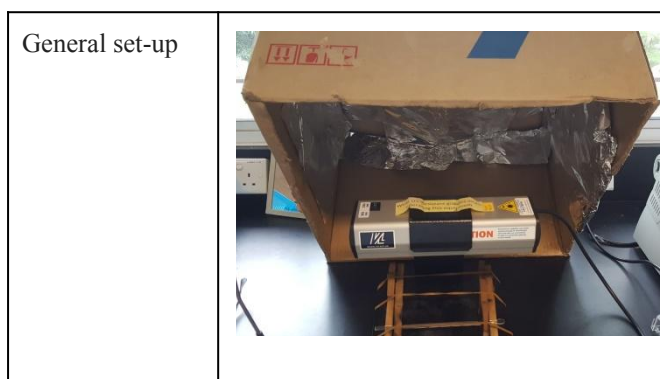
1.   Using a sonicator, 0.09 g of each catalyst was dispersed in 180cm3 of solvent A with 3 cm3 of agricultural cypermethrin to obtain a 0.5 g/dm3 solution of photocatalyst (Machuca-Martínez & Colina-Márquez, 2011).

2.   Then, each dispersed solution was separated into 15 10 cm3 volumetric flasks. These volumetric flasks are placed in the formation shown in Fig. 2 under a 324 nm UV light (Takahashi, et al., 1985).

3.   The set-up was covered with a cardboard box to ensure that the only source of light the reacting solutions is from the 324 nm UV lamp.

4.   Every 10 minutes up till 50 minutes, 3 volumetric flasks for each catalyst loading were removed and its contents were emptied into 3 separate centrifuge tubes, as 3 replicates.

5.   The solutions were then separately centrifuged for 5 minutes at 4000 RPM. Then, Beer lambert's law at 208 nm (Al-Shuja'a, et al., 2013) was to find the concentration in the solutions at each point in time, for each replicate.

4. Results and Discussion

4.1 Agricultural Cypermethrin purity

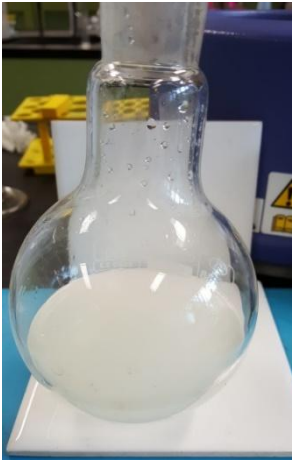Figure 3: Colour change during titration

Colour before titration	
Colour at end point	

Table 1: Trendlines from calibration curve in figure 4

Trendline:	Absorbance = 0.0052461[cypermethrin] + 0.0067096
Maximum Slope Trendline:	Absorbance = 0.0061311[cypermethrin] -0.010148
Minimum Slope Trendline:	Absorbance = 0.0044576[cypermethrin] + 0.025036

Solvent A's ethanol to water ratio was found to be 2:1. Ester hydrolysis in the fume hood caused a change in the solution's appearance from clear to a white emulsification appeared upon ester hydrolysis. This is caused by the 3-phenoxybezaldehyde formed, an ether with insufficient ethanol and water solubility (Ouellette & Rawn, 2015). On the other hand, the carboxylic acid formed is soluble in both ethanol and water due to its ability to from hydrogen bonds with the two solvents.

The addition of bromothymol blue (Fig. 3) after adding NaOH formed a blue solution, indicating the solution's alkalinity. During the titration, an average of 37.3 ± 0.1 cm3 of 0.25 mol dm-3 of HCl allowed the solution to reach its end point, indicated by the colour change to yellow. Therefore, from the back titration, the concentration of agricultural cypermethrin was calculated to be 3.075 ± 0.190 mol dm^{-3}.
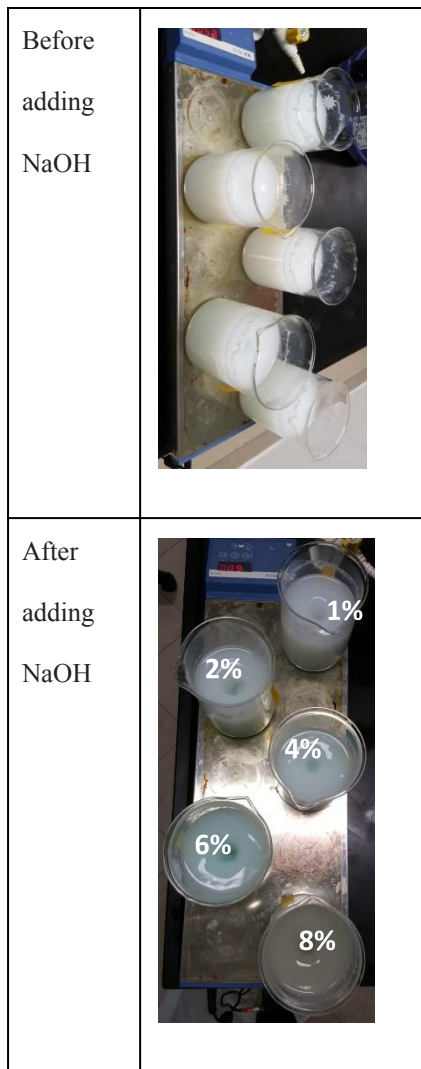
4.2 Calibration curve

Figure 4: Calibration curve at 208 nm for cypermethrin concentration in mmol dm^{-3}
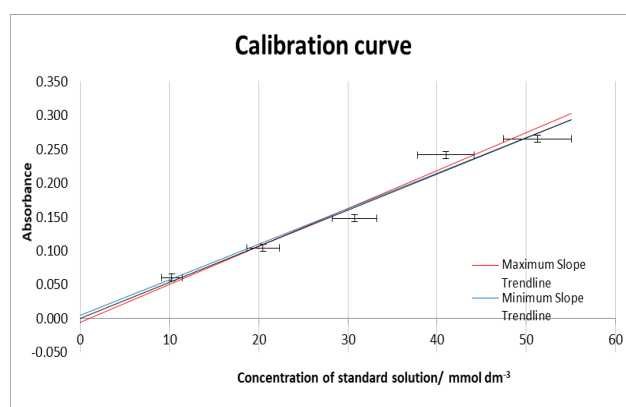
4.3 Synthesis and characterisation of catalysts

Figure 5: Catalyst synthesis solutions before and after adding NaOH

| Before adding NaOH	
After adding NaOH	

Prior to increasing pH to 10, all solutions were homogenous mixtures. Initially, due to the presence of Copper (II) ions, the solutions appeared blue. After 1 hour of stirring, all the solutions turned greyish white (ref. Fig. 5, top). The grey tinge suggests the formation of CuO to some degree. However, upon the addition of NaOH to change the pH of the solution to 10, there is an obvious colour change as precipitation immediately starts to form. The precipitates were of different colours from CuO loadings (ref. Fig. 5, bottom).

Figure 6: Post drying and calcination

Loading/w/w%	Photo

1	
2	
4	
6	
8	
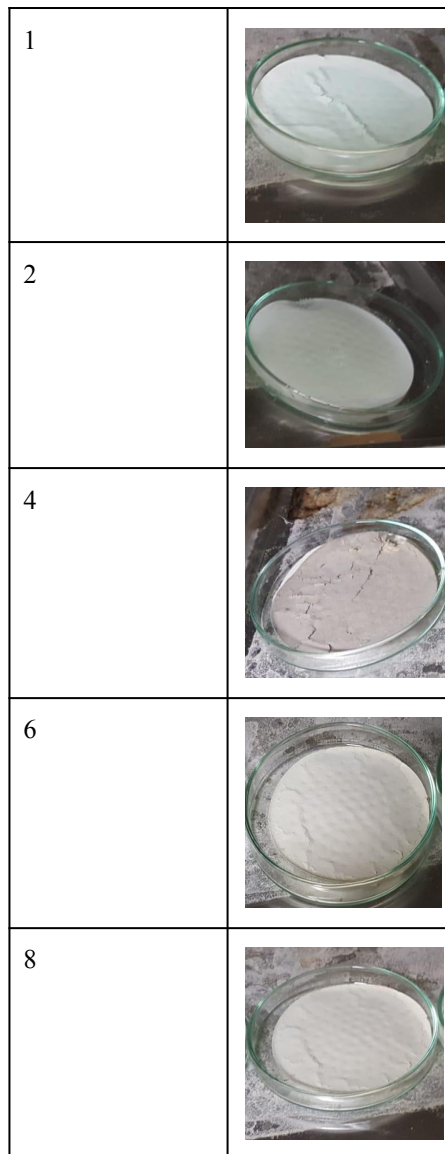
After filtering the solutions for the nanocomposites, the filter papers with solid catalysts were placed in an oven to dry and calcined in the furnace. The powdered catalysts obtained appear to have a greyer tinge than in Fig. 6. This is likely due to the heat in the calcination process converting any remaining $Cu(OH)_2$ into CuO, and forming the nanocomposite (Chen, et al., 2013).

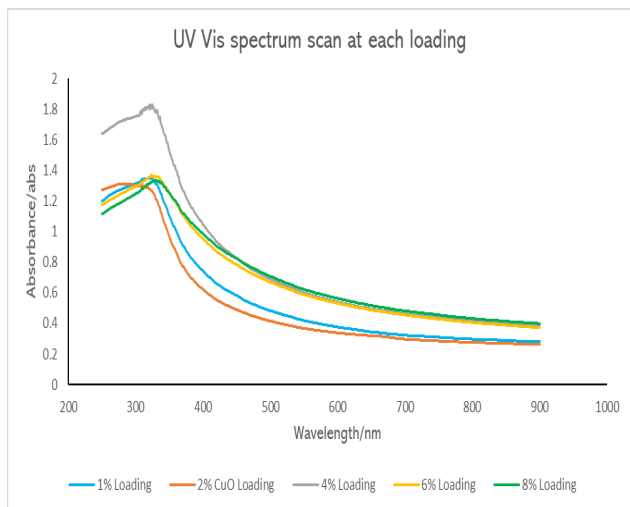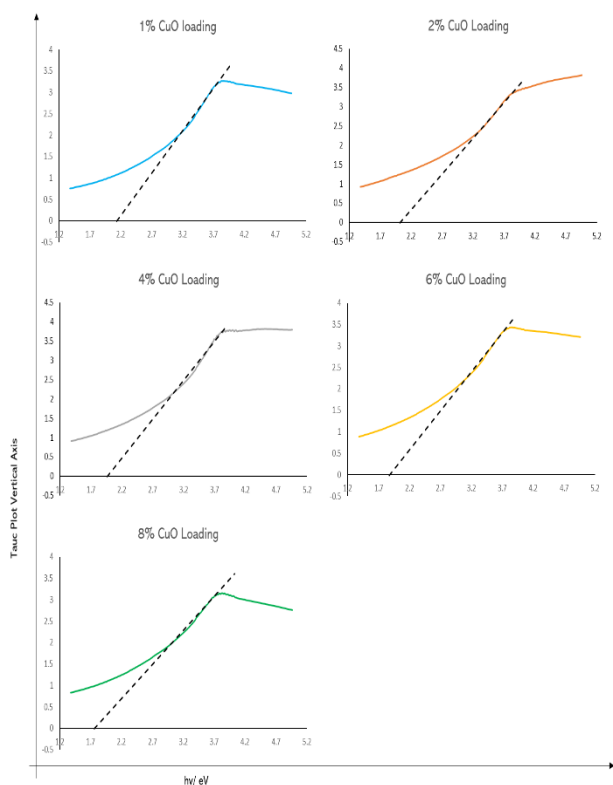Figure 7: UV Vis spectrum scan for each catalyst

Figure 8: Tauc Plots for each catalyst

In Fig. 7, the UV vis spectrum scan shows that the absorbance for each of the catalysts with CuO present have relatively high absorbance for the entire visible range, a sign that the nanoparticle has formed due to the nature of CuO to cause higher intensity absorption from 300 to 800 nm (Chen, et al., 2013). From the UV Vis spectrum scans, the following a Tauc plot at each loading was obtained as shown in Fig. 8.

Values for $(\alpha h v)^{\frac{1}{\gamma}}$ are plotted against hv for each CuO loading, resulting in irregularly shaped curves (Albert Zicko

Johannes, 2020) except for a linear section. This section is then extrapolated and this tangent's intersection with the horizontal axis is the band gap in eV.

The band gap of the control, pure anatase TiO_2 – at 0 w/w % CuO loading is 3.2 eV (Makula, et al., 2018) determined in previous literature. The band gaps obtained from the Tauc plot where the tangent intersects the horizontal axis in Fig. 7 is shown in Table 2:

Table 2: Band gaps of catalysts obtained from Tauc Plots

loading/ w/w %	band gap/ eV
1	2.14
2	2.03
4	1.97
6	1.88
8	1.76

As the percentage by weight loading (w/w %) of CuO increases, the band gap predictably decreases, a trend also observed in previous literature (Chen, et al., 2013). This occurs as the presence of CuO in anatase TiO_2 structure changes in the electronic state of Copper (II) in each of the catalysts, allowing electrons to move from the valence to conduction band using less energy. (Chen, et al., 2013)

4.4 Effect of catalysts on Cypermethrin degradation

At all loadings (ref Fig. 9), the photocatalytic degradation of cypermethrin in the presence of excess water is pseudo first order. This is reflected by all of the R^2 values of linear fit between ln[cypermethrin] and t exceeding 0.9. Thus, the pseudo first order rate constants, k, can be compared between different loadings.

Figure 9: Linear pseudo first order reaction graphs for each

catalyst
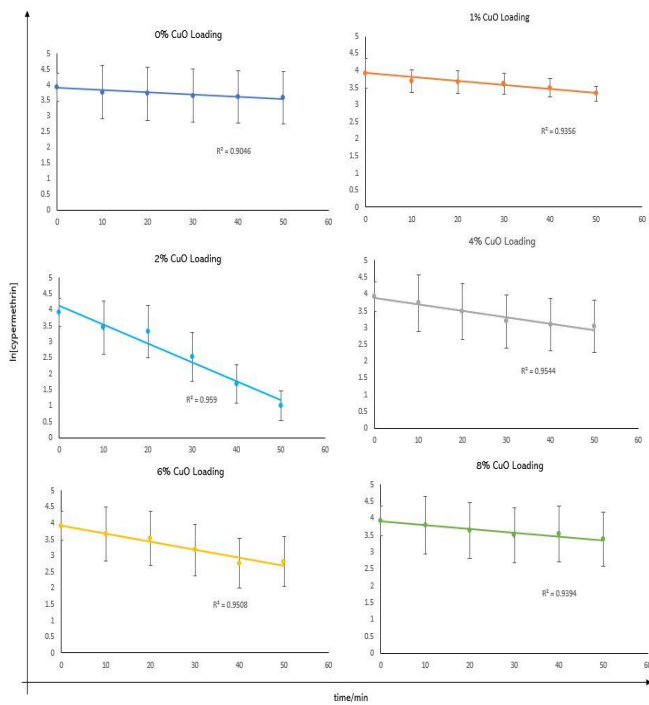
The linear plots like in Fig. 9 were obtained for all three replicates from appendix Table A5. All k values were the negative gradients of each of the plots (ref Equation 6) as cypermethrin decomposition occurs, incurring a reduction in the concentration of cypermethrin over time. The negative gradients from time-against-ln[cypermethrin] plots (k values) for each replicate is tabulated below:

Table 3: Gradients (k) of linear plots in mmol min dm^{-3}

w/w % CuO Loading	Rep. 1	Rep. 2	Rep. 3
0	0.0055	0.006194	0.006509
1	0.00953	0.010486	0.011289
2	0.05907	0.052653	0.045479
4	0.019173	0.01833	0.019749
6	0.023419	0.023557	0.02702
8	0.010812	0.010586	0.009827

An ANOVA t test (ref. Table 4) was conducted on rate constants in Table 3 with the following hypotheses:

H0: There is no statistically significant difference between CuO loadings and the rate constants (k) of cypermethrin decomposition

HA: There is a statistically significant difference between CuO loadings and the rate constants (k) of cypermethrin decomposition.

Table 4: ANOVA t test results for data in Table 3

Source of Variation	SS	df	MS	P-value
Between Groups	0.004345	5	0.000869	2.37E-09
Within Groups	0.000104	12	8.7E-06	
Total	0.00445	17		

HA is accepted as the p value is significantly lower than 0.05, suggesting that there is a substantially smaller probability than 0.05 that the differences in rate constants at various CuO loadings were merely from random variations in data. For a further analysis, a Tukey Post Hoc Test is conducted (table 5).

There is no statistically significant difference (p>0.05) between CuO loadings of 0 and 1w/w %; 0 and 8w/w %; and 4 and 6 w/w %. All other CuO loadings have statistically significant differences between them.

Table 5: Tukey Post Hoc Test results for data in table 3 (k values across replicates)

treatments pair (w/w % CuO Loading)	Tukey HSD Q statistic	Tukey HSD p-value	Tukey HSD inferfence
0% vs 1%	2.5641	0.493066	insignificant
0% vs 2%	27.2051	0.001005	** $p<0.01$
0% vs 4%	7.6427	0.001702	** $p<0.01$
0% vs 6%	10.9197	0.001005	** $p<0.01$
0% vs 8%	2.5485	0.498746	insignificant
1% vs 2%	24.641	0.001005	** $p<0.01$
1% vs 4%	5.0786	0.033863	* $p<0.05$
1% vs 6%	8.3556	0.001005	** $p<0.01$
1% vs 8%	0.0156	0.899995	insignificant
2% vs 4%	19.5624	0.001005	** $p<0.01$
2% vs 6%	16.2853	0.001005	** $p<0.01$
2% vs 8%	24.6565	0.001005	** $p<0.01$
4% vs 6%	3.277	0.259113	insignificant
4% vs 8%	5.0942	0.03324	* $p<0.05$
6% vs 8%	8.3712	0.001005	** $p<0.01$

Figure 10: Graph of average rate constant against CuO Loading in w/w % (Error bars obtained from standard deviation)
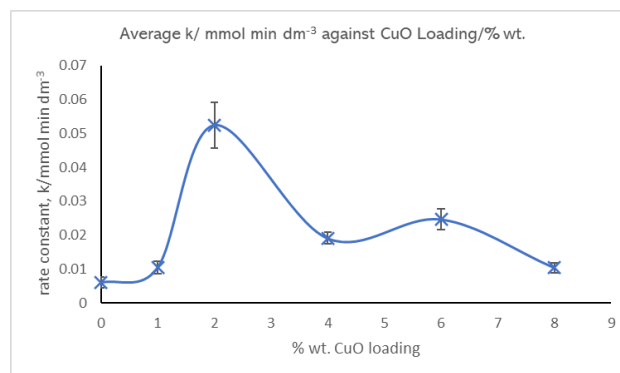
As the k value is proportional to the rate of cypermethrin decomposition (ref. Equation 6), the "effectiveness" of a catalyst refers to how high a k value it incurs. The catalyst is most effective at 2 w/w % CuO (ref Table 3 and Figure 10), and moderately effective between 4-6 w/w % CuO between which there is no significant difference. Above or below this narrow range, the effectiveness of CuO loading reduces to levels close to 0 w/w % loading, at which the slowest rate of cypermethrin degradation occurred.

Previous investigations applying CuO/ TiO$_2$ to other reactants suggests that there are two reasons for why this narrow range of CuO loading incurs the highest efficacy.

First, the higher the CuO loading, the lower the band gap (ref section 4.3) and thus the less energy from UV light is required for hydroxyl radicals to form from the excitation of electrons (ref section1.3). This reduces the activation energy for cypermethrin decomposition, increasing its rate (Michael Dahl, 2014). Thus, CuO loadings that are too low inhibit the efficacy of CuO/ TiO$_2$ catalysts.

Second, the higher loadings of CuO may cause CuO to accumulate on the TiO$_2$ surface, inhibiting the catalyst's porosity. This reduces the surface area of catalyst exposed to reactants (Jiang Wu, 2016), reducing its efficacy.

Therefore, a balance is required between reducing the band gap of TiO$_2$ and affecting TiO$_2$'s surface area in forming the nanocomposite. This balance occurs at 2 w/w % CuO loading.

5. Conclusion

In conclusion, nanocomposite catalysts of CuO loadings 1,2,4,6 and 8 w/w % have been successfully formed at low

cost as determined via UV Vis reflectance spectroscopy. The most effective loading was at 2 w/w % with the highest rate constant; it was the balance between having a low band gap while maintaining high porosity. Though this requires further investigation, the findings of this investigation may be used in the development of further at similar loadings for the mitigation of cypermethrin in agricultural soil after insecticide treatment to minimise water pollution in nearby water bodies.

7. Bibliography

1.   "Cypermethrin." National Centre for Biotechnology Information. PubChem Compound Database, U.S. National Library of Medicine, pubchem.ncbi.nlm.nih.gov/compound/Cypermethrin#section =2D-Structure).

2.   (IPCS), I. p. o. C. S., 1989. Environmental Health Critera 82 Cypermethrin, Geneva: United Nations Environment Programme; International Labour organization; World Health Organization.

3.   Ahmed, M. S., Sardar, M. M. A., Ahmad, M. & Kabir, K. H., 2017. Quantification of purity of some frequently used insecticides in vegetables insect pests. Asian Journal of Medical and Biological Research , pp. 267-275.

4.   Aktar, M. W., Sengupta, D. & Chowdhury, A., 2009. Impact of pesticides use in agriculture: their benefits and hazards. Interdisciplinary Toxicology, pp. 2(1): 1-12.

5.   Albert Zicko Johannes, R. K. P. a. M. B., 2020. Tauc Plot Software: Calculating energy gap values of organic materials based on Ultraviolet-Visible absorbance spectrum. IOP Conference Series: Materials Science and Engineering, Issue 823.

6.   Alemán, J. L. V. L. T. R. D. F. P. P. X. S. P. M. S. P. R. M. D. M. L. P. J., 2017. Visible-Light Photocatalytic Intramolecular Cyclopropane Ring Expansion. Angewandte Chemie (International Edition), a Journal of the German Chemical Society, pp. 7826-7830.

7.   Al-Shuja'a, O. M., Al-Kahali, M. S. N. & Dafa'e, B. A., 2013. Photodegradation of the Cypermethrin Form Insecticide "START" Induced by TiO2 in Aquatic Environment. Sana'a University Journal of Science & Technology, pp. 37-42.

8.   Ambrus, Á. & Hamilton, D., 2011. Evaluation of pesticide residues for estimation of maximum residue levels and calculation of dietary intake: Training manual, Rome: Food and Agricultural Organization of the United Nations.

9.   Anon., n.d. Cypermec 25 EC (100 ml). Hua Hng Trading Co Pte Ltd; World Farms Co Pte Ltd.

10.   Arabhosseini, A. & Faridi, H., 2018. Application of eggshell wastes as valuable and utilizable. Res. Agr. Eng., pp. 64: 104-114.

11.   Augustine Chioma Affam, M. C., 2013. Degradation of pesticides chlorpyrifos, cypermethrin and chlorothalonil in aqueous solution by TiO2 photocatalysis. Journal of Environmental Management, pp. 160-165.

12.   C.Cameselle, 2015. 8 - Electrokinetic remediation and other physico-chemical remediation techniques for in situ treatment of soil from contaminated nuclear and NORM sites. In: Environmental remediation and restoration of contaminated nuclear and norm sites. Cambridge, UK; Waltham, USA; Kidlington, UK: Woodhead publishing series in energy, pp. 161-184.

13.   Camilleri, P., 1984. Alkaline hydrolysis of some pyrethroid insecticides. Journal of Agricultural and Food Chemistry, pp. 32 (5), 1122-1124.

14.   Chapman, R. A., C. M. Tu, C. R. H. & Cole, C., 1981. Persistence of five pyrethroid insecticides in sterile and natural, mineral and organic soil. Bulletin of Environmental Contamination and Toxicology, p. 26: 513–519.

15.   Chen, W.-T.et al., 2013. The role of CuO in promoting photocatalytic hydrogen production over TiO2. International Journal of Hydrogen Energy, 38(35), pp. 15036-15048.

16.   Chen, X. et al., 2010. Investigation on solar photocatalytic activity of TiO2 loaded composite: TiO2/Eggshell, TiO2/Clamshell and TiO2/CaCO3. Materials letters, p. 64: 1437–1440.

17.   Chioma, A., Affam & MalayChaudhuri, 2013. Degradation of pesticides chlorpyrifos, cypermethrin and chlorothalonil in aqueous solution by TiO2 photocatalysis. Journal of environemtal science and management, pp. 160-165.

18.   Chrustek, A. et al., 2018. Current Research on the Safety of Pyrethroids Used as Insecticides. Medicina (Kaunas), p. 54(4): 61.

19.   Connor, N., 2019. What is Band Gap – Energy Gap in Semiconductors – Definition. Radiation Dosimetry, 14th December.

20.   Cycoń, M. & Piotrowska-Seget, Z., 2016. Pyrethroid-Degrading Microorganisms and Their Potential

for the Bioremediation of Contaminated Soils: A Review. Frontiers in Mircobiology, p. 7: 1463.

21.   Ekane Peter Etape, L. J. N. J. F.-T. ,. D. M. Y. ,. B. V. N., 2017. Synthesis and Characterization of CuO, TiO2, and CuO-TiO2 Mixed Oxide by a Modified Oxalate Route. Journal of Applied Chemistry.

22.   FO, O. et al., 2017. Remediation of Aqueous Solution of Cypermethrin and Chlorpyriphos Using Derived Adsorbent from Jatropha Curcas. J. Appl. Sci. Environ. Manage., pp. Vol. 21 (1) 40-46 .

23.   Gokul Dharan, J. H. K. S. J. D., 2018. University of Calgary, Energy Education, Conduction Band. [Online]

Available at:
https://energyeducation.ca/encyclopedia/Conduction_band

[Accessed 21 February 2021].

24.   health, M. D. o. c., revised 2005. Acetonitrile (CAS #75-05-8) Information for the Public.

25.   I.Al-Mughrabi, K., K.Nazer, I. & T.Al-Shuraiqi, Y., 1992. Effect of pH of water from the King Abdallah Canal in Jordan on the stability of cypermethrin. Crop Protection, pp. 4, 341-344.

26.   J.F.Artiola, J.L.Walworth, S.A.Musil & M.A.Crimmins, 2019. Chapter 14 - Soil and Land Pollution. In: Environmental and Pollution Science. s.l.:Elsevier Inc., pp. 219-235.

27.   Jiang Wu, C. L. X. C. J. Z. L. Z. T. H. H. C. Z. B. N. X. Z. P. L. W. Z., 2016. Photocatalytic oxidation of gas-phase Hg0 by carbon spheres supportedvisible-light-driven CuO–TiO2. Journal of Industrial and Engineering Chemistry.

28.   Jones, D., 1995. ENVIRONMENTAL FATE OF CYPERMETHRIN, Sacramento, CA 95814-3510: Environmental Monitoring & Pest Management.

29.   K.Malik, J., ManojAggarwal, StarlingKalpana & C.Gupta, R., 2017. Chapter 36 - Chlorinated Hydrocarbons and Pyrethrins/Pyrethroids. In: Reproductive and developemental toxicology (second edition). s.l.:Elsevier, pp. 633-655.

30.   Lina, L. et al., 2012. Degradation of cypermethrin, malathion and dichlorovos in water and on tea leaves with O3/UV/TiO2 treatment. Elsevier, pp. 374-379.

31.   LWendt-Rasch, Pirzadeh, P. & Woin, P., 2003. Effects of metsulfuron methyl and cypermethrin exposure on freshwater model ecosystems. Aquatic Toxicology , pp. 243-256.

32.   Machuca-Martínez, F. & Colina-Márquez, J. Á., 2011. Effect of the initial pH and the catalyst concentration on TiO2-based photocatalytic degradation of three commercial pesticides. Ingeniería y Desarrollo, pp. 84-100.

33.   Makula, P., Pacia, M. & Macyk, W., 2018. How To Correctly Determine the Band Gap Energy of Modified Semiconductor Photocatalysts Based on UV–Vis Spectra. J. Phys. Chem. Lett., pp. 9, 23, 6814–6817.

34.   Michael Dahl, Y. L. Y. Y., 2014. Composite Titanium Dioxide Nanomaterials. American Chemical Society, p. 9853–9889.

35.   Mugni, H. et al., 2011. Effect of Aquatic Vegetation on the Persistence of Cypermethrin Toxicity in Water. Bulletin of Environmental Contamination and Toxicology, pp. 86: 23-27.

36.   Onwubu, S. C., Mdluli, P. S. & Singh, S., 2019. Evaluating the buffering and acid-resistant properties of eggshell–titanium dioxide composite against erosive acids. Journal of applied biometrials and functional materials.

37.   ONWUBU, S. C., MDLULI, P. S., SINGH, S. & TLAPANA, T., 2019. A novel application of nano eggshell/titanium dioxide composite on occluding dentine tubules: an in vitro study. Brazilian Oral Research.

38.   Ouellette, R. J. & Rawn, J. D., 2015. 9 - Ethers and Epoxides. In: Principles of Organic Chemistry. s.l.:Elsevier, pp. 239-258.

39.   Palmquist, K., Salatas, J. & Fairbrother, A., 2011. Pyrethroid Insecticides. In: Insecticides: Advances in Integrated Pest Management. Rijeka, Coratia: InTech, pp. 251-252.

40.   Peh, C. K. N., Wang, X.-Q. & Ho, G. W., 2017. Increased photocatalytic activity of CuO/TiO2 through broadband solar absorption heating under natural sunlight. Procedia Engineering, Issue 215, pp. 171-179.

41.   Pizarro, R. A. S. & Barros, A. P. H., 2020. Cypermethrin elimination using Fe-TiO2 nanoparticles supported on coconut palm spathe in a solar flat plate photoreactor. Sage Journals.

42.   R.R.Stephenson, 1982. Aquatic toxicology of cypermethrin. I. Acute toxicity to some freshwater fish and invertebrates in laboratory tests. Aquatic Toxicology, pp. 175-185.

43.   Ridha, N. A.-S., Egzar, H. K. & Kamal, N. M., 2020. Synthesis and characterization of CuO nanoparticles and TiO2/CuO nanocomposite and using them as photocatalysts. AIP Conference Proceedings 2290, 030006.

44.   Rusmidah Ali, W. A. W. A. B. &. L. K. T., 2010. Zn/ZnO/TiO2 and Al/Al2O3/TiO2 Photocatalysts for the Degradation of Cypermethrin. CCSE modern applied science, Department of Chemistry, Faculty of Science Universiti Teknologi Malaysia.

45.   Shaheed, I. M. & Dhahir, S. A., 2020. Extraction and determination of alpha-Cypermethrin in environmental samples from Kerbala city / Iraq and in its formulation using high performance liquid chromatography (HPLC).. IOP Conference Series: Materials Science and Engineering.

46.   Stone, F. S., 1983. UV-Visible Diffuse Reflectance Spectroscopy Applied to Bulk and Surface Properties of Oxides and Related Solids. In: s.l.:s.n., pp. 273-272.

47.   TAKAHASHI, N., MIKAMI, N., MATSUDA, T. & MIYAMOTO, J., 1985. Hydrolysis of the Pyrethroid Insecticide Cypermethrin in Aqueous media. Journal of Pesticide Science, pp. 10, 643-648.

48.   Takahashi, N., Mikami, N., Matsuda, T. & Miyamoto, J., 1985. Photodegradation of the pyrethroid insecticide cypermethrin in water and on soil surfaces.. Journal of Pesticide Science, pp. 629-642.

49.   Temple, W. & Smith, N., 1996. Synthetic Pyrethroid Insecticides. Human Toxicology.

50.   Thi Hiep Nguyen, T. L. N. T. D. T. U. & Nguyen, Q. L., 2013. Synthesis and characterization of nano-CuO and CuO/TiO2 photocatalysts. Advances in Natural Sciences: Nanoscience and Nanotechnology.

51.   Tian, H., 2014. TiO2-supported copper nanoparticles prepared via ion exchange for photocatalytic hydrogen production. A thesis submitted for the degree of Masters by Research School of Chemical Engineering Faculty of Engineering The University of New South Wales Sydney, Australia.

52.   Ting-feng, L. et al., 2007. Effect of copper on the degradation of pesticides cypermethrin and cyhalothrin. Journal of environmetal sciences, pp. 1235-1238.

53.   Vignesh Kumaravel, M. D. I. A. B. R. K. C. J. Y. D. M. K. A. A.-W., 2019. Photocatalytic Hydrogen Production: Role of Sacrificial Reagents on the Activity of Oxide, Carbon, and Sulfide Catalysts. MDPI, Catalysts, p. 276: 35 pages.

54.   W., T. et al., 2018. Pyrethroid pesticide residues in the global environment: An overview.. PubMed, pp. 990-1007.

55.   Wakeling, E. N., Atchison, W. D. & Neal, A. P., 2012. Pyrethroids and their effects on Ion Channels. In: Pesticides - Advances in Chemical and Botanical Pesticides R.P. Soundararajan, IntechOpen, DOI: 10.5772/50330. s.l.:s.n.

56.   Wakeling, E. N., Neal, A. P. & Atchison, W. D., 2012. Pyrethroids and Their Effects on Ion Channels. In: Pesticides -- Advances in Chemical and Botanical Pesticides. s.l.:IntechOpen, p. chapter 3.

57.   Xie, J. et al., 2011. Photodegradation of lambda-cyhalothrin and cypermethrin in aqueous solution as affected by humic acid and/or copper: Intermediates and degradation pathways. Society of environmental toxicolgy and chemistry, pp. 2440-2448.

58.   Yates, K. & McClelland, R. A., 1967. Mechanisms of ester hydrolysis in aqueous sulfuric acids. J. Am. Chem. Soc., pp. 89, 11, 2686-2692.

59.   Y, N. et al., 2007. The in vitro metabolism of a pyrethroid insecticide, permethrin, and its hydrolysis products in rats.. Toxicology, pp. 235(3):176-84.

60.   Zhang, S. et al., 2020. CuO Nanoparticle-Decorated TiO2-Nanotube Heterojunctions for Direct Synthesis of Methyl Formate via Photo-Oxidation of Methanol. American Chemical Society, pp. 5, 26, 15942–15948.

8. Appendix

Table A1: Table of apparatus, chemicals and uncertainties

Measuring Equipment:	Other equipment:	Chemicals:
1.00 ± 0.01 cm^3 pipette 5.00 ± 0.05 cm^3 pipette 10.00 ± 0.02 cm^3 pipette 20.00 ± 0.06 cm^3 pipette 50.00 ± 0.5 cm^3 pipette 50.0 ± 0.1 cm^3 Burette - Stopwatch - UV Vis Spectrophotometer (±0.005 A; ±1 nm)	- Retort Stand - Round bottom flask - Rubber pipes - Condenser - Round bottom flask heater - Fume hood - Quartz Cuvette - Sonicator - Centrifuge 324 nm UV Lamp` - Cardboard box - Rubber bands - Wooden Tongs 10 cm^3 Volumetric flasks - Oven - Furnace (for calcination) - Filter paper - Vacuum Filter	95% ethanol - Agricultural cypermethrin solution 2 M NaOH 0.01 M H_2SO_4 0.25 M HCl - Bromothymol Blue Indicator - Distilled Water

Table A2: Table of variables

Type of Variable	Variable	Justification	Means of Measurement
Independent	CuO loading (1,2,4,6 and 8 w/w % by TiO_2) in photocatalyst	CuO loading affects the catalytic ability of TiO_2 and will thus affect the rate of cypermethrin decomposition.	Concentration of $Cu(NO_3)_2$ solution used in the synthesis of photocatalysts.
Dependent	Absorbance of reacting solution at 208 nm over time	The concentration of cypermethrin is proportional to absorbance eat 208nm. Thus, absorbance over time can be used to calculate rate of cypermethrin degradation in the presence of TiO_2 catalysts with the varying CuO loadings.	UV Vis spectroscopy will be used to measure absorbance, while a calibration curve will be used to convert absorbance to cypermethrin concentration.
Control	Initial cypermethrin concentration in reacting solution	As a pseudo first order reaction, the initial concentration of cypermethrin will affect the initial rate of decomposition of cypermethrin.	Volume of agricultural cypermethrin added to each volumetric flask with reacting solution is the same.
Control	Temperature	Temperature affects the kinetics of the particles and the activation energy present in the system. Thus, it may also affect rate of reaction and needs to be constant.	It is unrealistic to place temperature probes or thermometers in every single volumetric flask with reacting solution. However, the experiment was conducted in

			a temperature controlled laboratory set at 298 K.
Control	Wavelength of light from UV Lamp	These affect energy level of photons the photocatalyst is exposed to affecting rate of reactions.	Only the 324 nm UV lamp was used in experimentation. The reaction set-up is also covered by an opaque cardboard box during the run of the reaction, ensuing that the only light each solution receives is from the UV lamp.
Control	Light intensity of UV Lamp		It is unrealistic to place a light intensity probe over each volumetric flask. This would also obstruct the light received by each reacting solution. Thus, a light probe was placed in the middle of the UV lamp set-up over 5 minutes during which light intensity was found to remain relatively constant, especially due to the presence of the opaque cardboard box covering the set-up.

Table A3: Table of safety and ethical considerations

Source of Hazard	Hazard	Method to address hazard
Cypermethrin	Cypermethrin is dangerous when ingested, in direct contact with skin, and may release toxic fumes.	Cypermethrin reacting solutions used are diluted in solvent A in the fume hood. Reflux heating of cypermethrin was also conducted in the fume hood. Gloves were worn in the handling of the chemical.
Furnace	Dangerous to use due to high temperatures, may cause severe burns.	Substances to be calcined were given to the laboratory technician.
Oven		Heat resistant gloves were worn when operating the laboratory oven.
UV Lamp	Direct exposure to UV light may damage eyes.	Shaded safety goggles were worn while operating the UV lamp. A cardboard box was used to cover the reacting set-up as well.

Table A4: Absorbance data from cypermethrin calibration curve

Volume of agricultural cypermethrin solution in 60cm^3 of Solution A/ cm^3	Number of moles of cypermethrin solution in 60 cm^3 of solution A	[cypermethrin]/mm ol dm^{-3}	Abs. unc. of [cypermethrin]	Absorbance±0.005
1.00	0.00308	51.3	±3.83	0.266
0.80	0.00246	41.0	±3.17	0.242
0.60	0.00185	30.8	±2.50	0.148
0.40	0.00123	20.5	±1.84	0.104
0.20	0.00062	10.3	±1.18	0.060

Table A5: Raw absorbance data (orange) processed to concentration data (yellow) and linearized concentration data for linearized first order rate of reaction analysis (blue).

w/w % CuO	time/ min	Absorbance			Concentrations/ mmol dm^{-3}			Linear plot (ln[Cypermethrin])		
		Rep. 1	Rep. 2	Rep. 3	Rep. 1	Rep. 2	Rep. 3	Rep. 1	Rep. 2	Rep. 3
0	0	--	--	--	50.4	50.4	50.4	3.92	3.92	3.92
	10	**0.234**	0.243	0.225	**43.3**	45.0	41.6	**3.77**	3.81	3.73
	20	0.230	0.231	0.208	42.6	42.8	38.4	3.75	3.76	3.65
	30	0.208	0.216	0.206	38.4	39.9	38.0	3.65	3.69	3.64
	40	0.212	0.198	0.199	39.1	36.5	36.7	3.67	3.60	3.60
	50	0.202	0.204	0.188	37.2	37.6	34.6	3.62	3.63	3.54
1	0	--	--	--	50.4	50.4	50.4	3.92	3.92	3.92
	10	0.209	0.225	0.214	38.6	41.6	39.5	3.65	3.73	3.68
	20	0.216	0.216	0.198	39.9	39.9	36.5	3.69	3.69	3.60
	30	0.207	0.203	0.19	38.2	37.4	34.9	3.64	3.62	3.55
	40	0.178	0.175	0.181	32.7	32.1	33.2	3.49	3.47	3.50
	50	0.158	0.157	0.141	28.8	28.6	25.6	3.36	3.36	3.24
2	0	--	--	--	50.4	50.4	50.4	3.92	3.92	3.92
	10	0.171	0.167	0.163	31.3	30.6	29.8	3.44	3.42	3.39
	20	0.153	0.141	0.141	27.9	25.6	25.6	3.33	3.24	3.24
	30	0.072	0.068	0.064	12.4	11.7	10.9	2.52	2.46	2.39
	40	0.035	0.039	0.055	5.4	6.2	9.2	1.69	1.82	2.22

	50	0.021	0.027	0.033	2.7	3.9	5.0	1.00	1.35	1.61
	0	--	--	--	50.4	50.4	50.4	3.92	3.92	3.92
	10	0.235	0.219	0.221	43.5	40.5	40.8	3.77	3.70	3.71
	20	0.169	0.185	0.177	30.9	34.0	32.5	3.43	3.53	3.48
	30	0.140	0.132	0.127	25.4	23.9	22.9	3.24	3.17	3.13
	40	0.122	0.124	0.12	22.0	22.4	21.6	3.09	3.11	3.07
4	50	0.115	0.119	0.111	20.6	21.4	19.9	3.03	3.06	2.99
	0	--	--	--	50.4	50.4	50.4	3.92	3.92	3.92
	10	0.221	0.220	0.195	40.8	40.7	35.9	3.71	3.71	3.58
	20	0.190	0.176	0.192	34.9	32.3	35.3	3.55	3.47	3.56
	30	0.140	0.132	0.124	25.4	23.9	22.4	3.24	3.17	3.11
	40	0.098	0.094	0.078	17.4	16.6	13.6	2.86	2.81	2.61
6	50	0.098	0.099	0.085	17.4	17.6	14.9	2.86	2.87	2.70
	0	--	--	--	50.4	50.4	50.4	3.92	3.92	3.92
	10	0.242	0.241	0.237	44.9	44.7	43.9	3.80	3.80	3.78
	20	0.209	0.196	0.213	38.6	36.1	39.3	3.65	3.59	3.67
	30	0.182	0.183	0.175	33.4	33.6	32.1	3.51	3.51	3.47
	40	0.188	0.178	0.189	34.6	32.7	34.7	3.54	3.49	3.55
8	50	0.156	0.161	0.166	28.5	29.4	30.4	3.35	3.38	3.41